

This work was written as part of one of the author's official duties as an Employee of the United States Government and is therefore a work of the United States Government. In accordance with 17 U.S.C. 105, no copyright protection is available for such works under U.S. Law.

Public Domain Mark 1.0

<https://creativecommons.org/publicdomain/mark/1.0/>

Access to this work was provided by the University of Maryland, Baltimore County (UMBC) ScholarWorks@UMBC digital repository on the Maryland Shared Open Access (MD-SOAR) platform.

Please provide feedback

Please support the ScholarWorks@UMBC repository by emailing scholarworks-group@umbc.edu and telling us what having access to this work means to you and why it's important to you. Thank you.

PROCEEDINGS OF SPIE

[SPIDigitalLibrary.org/conference-proceedings-of-spie](https://spiedigitallibrary.org/conference-proceedings-of-spie)

Remote sensing techniques to monitor nitrogen-driven carbon dynamics in field corn

Lawrence Corp, Elizabeth Middleton, Petya K. Campbell, K. Fred Huemmmrich, Yen-Ben Cheng, et al.

Lawrence A. Corp, Elizabeth M. Middleton, Petya K. Entcheva Campbell, K. Fred Huemmmrich, Yen-Ben Cheng, Craig S. T. Daughtry, "Remote sensing techniques to monitor nitrogen-driven carbon dynamics in field corn," Proc. SPIE 7454, Remote Sensing and Modeling of Ecosystems for Sustainability VI, 745403 (20 August 2009); doi: 10.1117/12.825508

SPIE.

Event: SPIE Optical Engineering + Applications, 2009, San Diego, California, United States

Remote sensing techniques to monitor nitrogen-driven carbon dynamics in field corn

Lawrence A. Corp¹, Elizabeth M. Middleton², Petya K. Entcheva Campbell³,
K. Fred Huemmrich³, Yen-Ben Cheng⁴, Craig S.T. Daughtry⁵

¹Sigma Space Corporation, Lanham, MD 20706

²Biospheric Sciences Branch, NASA/GSFC, Greenbelt, MD 20771

³Joint Center for Earth Systems Technology, UMBC, Baltimore, MD 21250

⁴Earth Resources Technology Incorporated, Annapolis Junction, MD 20701

⁵Hydrology & Remote Sensing Laboratory, USDA ARS, Beltsville, MD, 20705

ABSTRACT

Patterns of change in vegetation growth and condition are one of the primary indicators of the present and future ecological status of the globe. Nitrogen (N) is involved in photochemical processes and is one of the primary resources regulating plant growth. As a result, biological carbon (C) sequestration is driven by N availability. Large scale monitoring of photosynthetic processes are currently possible only with remote sensing systems that rely heavily on passive reflectance (R) information. Unlike R, fluorescence (F) emitted from chlorophyll is directly related to photochemical reactions and has been extensively used for the elucidation of the photosynthetic pathways. Recent advances in passive fluorescence instrumentation have made the remote acquisition of solar-induced fluorescence possible. The goal of this effort is to evaluate existing reflectance and emerging fluorescence methodologies for determining vegetation parameters related to photosynthetic function and carbon sequestration dynamics in plants. Field corn N treatment levels of 280, 140, 70, and 0 kg N / ha were sampled from an intensive test site for a multi-disciplinary project, Optimizing Production Inputs for Economic and Environmental Enhancement (OPE). Aircraft, near-ground, and leaf-level measurements were used to compare and contrast treatment effects within this experiment site assessed with both reflectance and fluorescence approaches. A number of spectral indices including the R derivative index D_{730}/D_{705} , the normalized difference of R_{750} vs. R_{705} , and simple ratio R_{800}/R_{750} differentiated three of the four N fertilization rates and yielded high correlations to three important carbon parameters: C:N, light use efficiency, and grain yield. These results advocate the application of hyperspectral sensors for remotely monitoring carbon cycle dynamics in terrestrial ecosystems.

Keywords: Remote Sensing, Vegetation, Reflectance, Fluorescence, Carbon, Nitrogen

1. INTRODUCTION

A major goal of the U.S. Carbon Cycle Science Program is to monitor the vegetation processes related to carbon dioxide (CO₂) uptake. Biological carbon (C) sequestration is driven by nitrogen (N) availability since N is a key component in photochemical enzymes and light harvesting pigments. Large scale monitoring of vegetation processes are currently possible only with remote sensing systems that rely heavily on passive reflectance (R) information. R indices particularly in the red edge have demonstrated significant relationships to leaf and canopy chlorophyll (Chl) content^[1]. Fluorescence (F) emitted from chlorophyll has been extensively used for the elucidation of the photosynthetic pathways and is more directly linked to photochemical reactions. However, remote utilization of the relatively weak F signal in C cycle science has been elusive. Recent advances in high resolution spectral radiometers have enabled mathematical manipulations based on the Fraunhofer Line Depth (FLD) principle to isolate the solar induced F (SIF) signal from the high resolution R continuum^[2-7]. Here we will present multi-year data describing leaf and canopy biophysical changes induced by N driven C cycling in corn (*Zea mays* L.) and present considerations for both F and R sensing methodologies to remotely quantify key regulators of ecosystem/biome productivity.

Agricultural studies of foliar chemistry, including N content, have been crop specific, such as studies on corn^[8,9], cotton^[10], and wheat^[11]. These studies have shown a number of correlations between various parts of the reflected spectrum and leaf N status. Leaves that are stressed tend to have lower chlorophyll concentrations causing an increase in reflectance in the visible and the infrared (IR). Asner and Vitousek^[12] describe how they used AVIRIS to estimate canopy N and water content in Hawaiian forests. Corn crops are among the highest consumers of N fertilizers in the United States and a rapid quantitative measure of N status for this crop would prove useful to many farming systems where substantial investments are made in the application of N fertilizers. A rapid non-destructive assessment of leaf N would be useful in determining problem spots in fields where organic or chemical supplements may improve soil fertility and crop yield while reducing the potential for contamination of surface and ground waters.

Here we will evaluate vegetation R indices and demonstrate successful methods to extract passive SIF from high resolution reflectance spectra and apply this information at canopy and ecosystem scales to provide more accurate assessments of gross primary productivity (GPP). Specific objectives of this study were designed to: (1) perform a biophysical summary of N driven C uptake in field corn; (2) present an approach to scale leaf photosynthetic gas exchange to simulate canopy C uptake as a function of canopy LAI and leaf N content; (3) determine if viable SIF can be obtained within the telluric O₂ absorption bands from field R spectra and aircraft multi-spectral R imagery of terrestrial vegetation assemblages; (4) compare the ability of R and FLD derived F indices at several observation levels to discriminate experimental vegetation treatments and identify relationships to biophysical manifestation of N driven C uptake.

2. MATERIALS AND METHODS

The experiment site located at USDA Beltsville Agricultural Research Center is part of an intensive multi-disciplinary project, Optimizing Production Inputs for Economic and Environmental Enhancement (OPE3). An intensive ground sampling protocol was initiated in 2001 across the N test site and within an adjacent wooded riparian wetland. The corn N test site consisted of 12 plots large enough to capture the spatial variability of crop and soil parameters with treatment groups of 280, 140, 70, and 0 kg N / ha, which provided a range of plant growth and condition. Leaf and crop biophysical parameters along with canopy R were acquired at the grain fill (R3) reproductive stage. These measurements included pigment contents, leaf optical properties, total leaf C:N, and maximum photosynthetic rate (A_{\max}). *In situ* geo-referenced canopy measurements were comprised of leaf area index (LAI), light use efficiency (LUE, ϵ), grain yield (kg/ha), and canopy R. Measurements from 2001 to 2007 occurred *in situ* where possible, otherwise uppermost fully expanded leaves (3rd leaf from terminal) were excised from the plant canopy.

2.1 Biophysical Observations

Leaf photosynthetic capacity (A_{\max}) was determined *in situ* with the LI-6400 photosynthetic system (LI-COR Biosciences, Lincoln, NE). A_{\max} was determined under controlled conditions of 1660 $\mu\text{mol m}^{-2} \text{s}^{-1}$ PAR, saturating CO₂ concentration (1000 ppm), controlled leaf temperature (22°C), and relative humidity (~35%). LUE was calculated as the ratio of C secured by vegetation per unit of absorbed photosynthetic active radiation (*a*PAR) as determined from leaf optical properties with an ASD spectral-radiometer (FieldSpec Pro, Analytical Spectral Devices, Inc., Boulder, CO) coupled to the LI-1800 Integrating sphere. The plant gas exchange simulator (PGES) is a comprehensive graphical user interface driven leaf/canopy gas exchange model that used key environmental variables such as LAI, PAR, CO₂, air temperature, relative humidity, wind speed, and soil moisture on maize to scale from the leaf A_{\max} observations to canopy gas exchange A_{net} . Canopy fraction of absorbed PAR (*fa*PAR_c) was derived from LAI measurements using the Beer-Lambert law with the light extinction coefficient *k* set to 0.55, the default value for modern hybrid corn^[13].

2.2 Spectral Reflectance

The ASD spectral-radiometer was also used to measure canopy radiance 1 m above plant canopies with a 22° field of view and a 0° nadir view zenith angle. A second cross-calibrated ASD radiometer was used in a similar viewing geometry over a Spectralon reference panel (Labsphere, North Sutton, NH) to simultaneously track changes in solar irradiance. The ASD FR spectral-radiometer covers the spectral range of 350 – 1000 nm with a 512 channel silicon photodiode array overlaid with an order separation filter to provide a 3 nm Full-Width at Half Maximum (FWHM) spectral resolution with a 1 nm sampling interval. Two separate, thermal electrically cooled InGaAs photodiodes are used to cover the spectral range of 1000 - 2500 nm at a 10 nm FWHM spectral resolution. Measurements were obtained on a clear day in a two-hour window around solar noon yielding an average PPFD of 1660 $\mu\text{mol m}^{-2} \text{s}^{-1}$. Aircraft multispectral R imagery was acquired in 2001 and 2004 with the Airborne Imaging Spectrometer for Applications

(AISA, flown by 3DI LLC, Easton MD). The AISA imaging spectrometer was configured with 35 bands ranging from 420 nm to 884 nm each with a spectral resolution of 1.6 nm FWHM. The instrument was flown at 2,500 m with an instantaneous field of view of 1 mrad yielding a 2.5 m per pixel ground resolution.

2.3 FLD Derived SIF

An adaption of the classic FLD approach^[14] was applied to canopy R spectra and AISA imagery to discriminate the relatively weak *in situ* vegetation F in-fill of the telluric O₂ bands that fall within the SIF region. The major telluric oxygen features are located at 688 nm (O_{2β}) and 760 nm (O_{2α}) with the observed FWHM and band depth of each feature highly dependent on spectrometer resolution and sampling interval. The FLD method is based on the differential absorption between the radiance measured in the well of an absorption feature at λ_d and a reference band just outside the feature λ_c. R and F at λ_d can be resolved by the solution of the following two equation system:

$$R_d = (c-d)/(a-b) \quad (7)$$

$$F_d = d - R_b = (ad - cb)/(a-b) \quad (8)$$

Here 'a' and 'b' represent the reference panel radiance in and out of each O₂ feature, respectively, and 'c' and 'd' represent the target radiance^[2]. This formulation of the FLD method assumes that both R and F are constant between λ_c and λ_d. To avoid inaccuracies associated with this assumption, the FLD algorithm was modified with absorption feature analysis and continuum removal to adjust the within feature variables 'b' and 'd' by making use of multiple wavebands from high resolution spectra^[15,16]. F within a Fraunhofer feature can also be expressed as the relative stationary yield ($f = F_d/a$), a dimensionless number representing the degree to which radiance within a relatively dark Fraunhofer line is augmented.

2.2 Diurnal Spectral Observations and Gas Exchange

An optical breadboard was configured to enable simultaneous *in situ* measurements of corn leaf photosynthetic gas exchange (A_{net}) with the LI-6400 and nearby adaxial spectral observations with the ASD spectral-radiometer (Fig. 1). Conditions within the photosynthesis chamber were established to track actual changes in the external environment for PAR, temperature, and relative humidity. The optical breadboard was attached to a tripod and adjusted to maintain direct solar illumination over the course of the day and maintain a 15° off NADIR sensor view angle. A Spectralon panel was briefly placed in front of the leaf for paired leaf and solar radiance measurements. Measurements were collected from sunrise to sunset on five separate leaves fertilized at 140 kg N /ha during the reproductive growth phases R3 to R5.

2.3 Computation of R spectral indices

A number of R indices were evaluated based on consistent performance over measurement scales and reproducible correlations to biophysical measures of plant growth and condition. Of the R indices surveyed the equations defining top performing R indices are summarized in Table 1. These equations were applied to R spectra at the leaf, canopy, and aircraft observation levels. A Gaussian 1nm FWHM spectral re-sampling procedure was applied to the AISA multispectral imagery to match the sampling frequency of the ASD spectral-radiometer over the wavelength range of 500 to 900 nm.



Fig. 1 Optical configuration for *in situ* photosynthesis and adaxial reflectance.

Table 1. Reflectance spectral indices identified as exhibiting significant relationships to corn growth and condition at leaf, canopy, and aircraft observation levels.

Spectral Index	Category	Reference
$CI_{red-edge} = (R_{770-800}/R_{720-730}) - 1$	Chlorophyll Reflectance Index	[17]
D_{730}/D_{705}	Red Edge Derivative Index	[18]
D_{max}/D_{705}	Red Edge Derivative Index	[18]
D_{max}/D_{744}	Derivative Ratio	[19]
$EVI = 2.5(R_{840-875} - R_{620-670})/(R_{840-875} + 6R_{620-670} + 1)$	Enhanced Vegetation Index	[20]
$ND_{705} = (R_{750} - R_{705})/(R_{750} + R_{705})$	Red Edge Index	[21]
$PRI_{550} = (R_{550} - R_{531})/(R_{550} + R_{531})$	Photochemical Reflectance Index	[22]
R_{740}/R_{720}	Simple Ratio	[23]

4. RESULTS

4.1 Biophysical Summary of Field Corn Growth

Multi-year analysis (2001 to 2007) of field corn growth indicated that leaf parameters (Chl, N, GPP_l , ϵ_l) and crop parameters (GPP_c , $fPAR_c$, grain yield, ϵ_c) increased with N level (Table 2). Foliar N content increased with application rate with the ANOVA model discriminating the four treatment levels at a minimum significant difference of 0.084 g m^{-2} . The remaining foliar parameters (Chl, C:N, GPP_l , and ϵ_l) were similar for the two N fertilization rates $\geq 140 \text{ kg N/ha}$, while significant decreases were obtained for treatments $\leq 70 \text{ kg N/ha}$. The canopy parameters all exhibited similar trends with higher values as N level increased, and with significant decreases for treatments $\leq 70 \text{ kg N/ha}$. Agreement between the measured ϵ_l and PGES modeled ϵ_c relative to a 1:1 line is shown in Figure 2. In general, the PGES model provided higher estimates of LUE than actual measurements which is attributed to saturating CO_2 conditions in the measurement chamber not inducing the theoretical A_{max} predicted by the model. Overall, the analysis of corn growth and condition indicates the recommended N application rate of 140 kg N/ha was optimal for corn grown at this location on a sandy loam soil while lowering the application rate produced crop symptoms consistent with N deficiency.

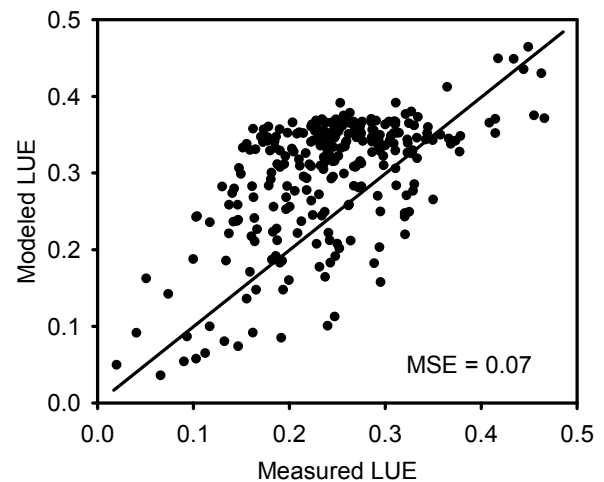


Fig. 2. Agreement between the measured leaf light use efficiency (ϵ_l) and PGES modeled leaf light use efficiency expressed as $\mu\text{g C per } \mu\text{mole of } aPAR$.

Table 2. Multi-year analysis of leaf (l) and canopy (c) biophysical parameters as a function N application rate.

Application (kg N/ha)	Chl (g/m^2)	N (g/m^2)	C:N	GPP_l^*	$\epsilon_l^\#$	GPP_c^*	$fPAR_c$	$\epsilon_c^\#$	Yield (Mg/ha)
280	0.58 a [†]	1.97 a	14.9 a	500 a	0.34 a	784 a	0.77 a	0.62 a	7.23 a
140	0.55 a	1.88 b	15.8 a	493 a	0.33 a	772 a	0.76 a	0.61 a	7.10 a
70	0.48 b	1.62 c	17.8 b	454 b	0.31 b	695 b	0.73 b	0.57 b	5.94 b
0	0.29 c	1.12 d	25.6 c	298 c	0.22 c	413 c	0.64 c	0.39 c	3.78 c
LSD _{.05}	0.025	0.084	1.04	19.2	0.014	31.7	0.016	0.023	0.277

[†]Column-wise mean values (n=265 to 325) represent analysis corn growth parameters taken in the reproductive development stages from 2001 to 2007. Means with the same letter are not separable by a repeated measures mixed model ANOVA_{LSD.05}.

[#]Leaf (ϵ_l) and canopy (ϵ_c) light use efficiency is expressed as $\mu\text{g C per } \mu\text{mole of absorbed photosynthetically active radiation}$.

*Mid-day gross primary productivity (GPP) is expressed as $\mu\text{g C m}^{-2} \text{ s}^{-1}$.

4.3 Spectral Remote Sensing of C Parameters with Reflectance

A number of R indices surveyed from the literature and developed by members of this group were evaluated based on consistent performance over measurement scales and reproducible correlations to biophysical measures of plant growth and condition. Table 1 summarizes the spectral indices surveyed in this study for differentiating plant growth and condition as induced by varying N application rates. Table 3 identifies significant correlations between the reported indices calculated from leaf, canopy, and aircraft spectral data to LUE, C:N, and yield. The derivative index D_{730}/D_{705} and the normalized difference index ND_{705} produced consistently high levels of association to physical measures of growth over the three observation levels. The R derivative index D_{max}/D_{744} also performed well, yielding the highest correlations of the indices surveyed to the carbon parameters C:N ($r=0.90$) and LUE ($r=-0.88$) at the near canopy observation level but was not as efficient at the leaf and aircraft observations. PRI_{550} , which is commonly used as a remotely sensed indicator of LUE in plant canopies, performed modestly at the leaf and aircraft levels and was ineffective in the near canopy observations.

The ANOVA $LSD_{0.05}$ model was used to assess the ability of spectral indices to differentiate the four N treatments at the leaf (Table 4a), canopy (Table 4b), and aircraft (Table 4c) observation levels. The leaf spectral indices $CI_{red-edge}$, D_{730}/D_{705} , and R_{740}/R_{720} were similar for the two N fertilization rates ≥ 140 kg N/ha, while significant decreases were obtained for treatments ≤ 70 kg N/ha. The PRI_{550} index exhibited superior performance, differentiating all four fertilization rates with a minimum significant index difference of 0.0032 (Table 4a). Performance of the PRI_{550} index decreased at canopy and aircraft observation levels while the performance of the remaining indices improved. At the ASD canopy observation level the $CI_{red-edge}$ and D_{730}/D_{705} spectral indices outperformed the remaining indices with minimum significant index differences of 0.076 and 0.108 respectively (Table 4b). At the AISA aircraft observation level all the reported spectral R indices, with the exception of PRI_{550} , differentiated the four N application rates (Table 4b). These observations imply that N induced changes in leaf physiology combined with changes in canopy structure (f_aPAR , Table 2) contributed to steady improved index performance from leaf to aircraft observation levels.

Table 3. Pearson correlation coefficients (R) indicate significant relationships exist between spectral indices and physiological measures of plant growth at leaf, near-field canopy, and far-field aircraft measurement scales.

R Index	LUE [†]			C:N			Yield		
	Leaf	Canopy	AISA	Leaf	Canopy	AISA	Leaf	Canopy	AISA
$CI_{red-edge}$	0.75*	0.77	0.76	-0.77	-0.81	-0.80	0.75	0.83	0.78
D_{730}/D_{705}	0.75	0.80	0.79	-0.77	-0.84	-0.81	0.79	0.85	0.79
D_{max}/D_{705}	0.66	0.73	0.78	-0.68	-0.77	-0.81	0.71	0.82	0.79
D_{max}/D_{744}	-0.72	-0.88	-0.75	0.73	0.90	0.80	-0.68	-0.73	-0.76
EVI	0.59	0.68	0.76	-0.59	-0.74	-0.79	0.43	0.73	0.77
ND_{705}	0.74	0.78	0.79	-0.76	-0.82	-0.81	0.70	0.76	0.78
PRI_{550}	0.71	0.36	0.73	-0.73	-0.37	-0.74	0.71	0.38	0.68
R_{740}/R_{720}	0.75	0.76	0.77	-0.77	-0.81	-0.80	0.76	0.81	0.78
SIF_{760}	na	0.42	0.54	na	-0.51	-0.74	na	0.53	0.73
SIF_{RFR}	na	-0.46	-0.62	na	0.56	0.77	na	-0.56	-0.79

[†]Midday light use efficiency (LUE) was used for leaf (ϵ_l) while for canopy and aircraft observations ϵ_c was used.

*Strength of association t-test probability coefficients ($p < 0.01$) otherwise relationship was deemed not significant (ns).

#Band not available (na).

Table 4a. Leaf spectral indices to differentiate N treatment effects on field corn growth.

Treatment (kg N/ha)	CI _{red-edge}	D ₇₃₀ /D ₇₀₅	D _{max} /D ₇₄₄	EVI	ND ₇₀₅	PRI ₅₅₀	R ₇₄₀ /R ₇₂₀	SIF ₇₆₀	SIF _{RFR}
280	0.88 a [†]	1.50 a	3.37 a	0.80 a	0.50 a	-0.062 a	1.62 a	na	na
140	0.88 a	1.48 a	3.06 a	0.79 ab	0.49 ab	-0.065 b	1.62 a	na	na
70	0.81 b	1.27 b	3.19 a	0.76 b	0.48 b	-0.069 c	1.56 b	na	na
0	0.60 c	0.81 c	5.70 b	0.68 c	0.40 c	-0.080 d	1.39 c	na	na
LSD _{.05}	0.051	0.115	0.678	0.031	0.021	0.0032	0.042	na	na

Table 4b. Canopy spectral indices to differentiate N treatment effects on field corn growth.

Treatment (kg N/ha)	CI _{red-edge}	D ₇₃₀ /D ₇₀₅	D _{max} /D ₇₄₄	EVI	ND ₇₀₅	PRI ₅₅₀	R ₇₄₀ /R ₇₂₀	SIF ₇₆₀	SIF _{RFR}
280	1.77 a [†]	2.61 a	1.37 a	1.23 ab	0.645 a	-0.081 a	2.09 a	5.00 a	0.92 a
140	1.68 b	2.43 b	1.47 ab	1.24 a	0.640 ab	-0.086 b	2.04 a	4.71 a	1.00 a
70	1.54 c	2.27 c	1.57 b	1.19 b	0.623b	-0.087 b	1.97 b	4.23 b	1.13 b
0	0.94 d	1.32 d	2.57 c	0.90 c	0.48 c	-0.097 c	1.58 c	2.48 c	1.53 c
LSD _{.05}	0.076	0.108	0.118	0.050	0.019	0.0023	0.049	0.29	0.13

Table 4c. AISA aircraft spectral indices to differentiate N treatment effects on field corn growth.

Treatment (kg N/ha)	CI _{red-edge}	D ₇₃₀ /D ₇₀₅	D _{max} /D ₇₄₄	EVI	ND ₇₀₅	PRI ₅₅₀	R ₇₄₀ /R ₇₂₀	SIF ₇₆₀	SIF _{RFR}
280	1.72 a [†]	2.77 a	1.04 a	0.85 a	0.59 a	-0.033 a	2.17 a	3.82 a	0.178 a
140	1.64 b	2.65 b	1.06 b	0.82 b	0.58 b	-0.035 a	2.12 b	3.69 a	0.197 b
70	1.40 c	2.25 c	1.09 c	0.74 c	0.54 c	-0.043 b	1.97 c	3.22 b	0.273 c
0	1.09 d	1.78 d	1.13 d	0.62 d	0.47 d	-0.050 c	1.75 d	2.48 c	0.433 d
LSD _{.05}	0.046	0.068	0.0067	0.019	0.009	0.0020	0.032	0.15	0.007

[†]Column-wise mean values represent a combined analysis of several years (2001-2007) of corn growth parameters in the R1-R3 reproductive development stages. Means with the same letter are not separable by a repeated measures mixed model ANOVA_{LSD,0.05}.

4.4 FLD Retrieval of SIF

The modified FLD algorithm applied to multiple years of canopy radiance spectra acquired with the ASD spectral-radiometer was able to provide F retrievals from the O₂ absorption feature in the range of 2 to 6 mWm⁻²nm⁻¹sr⁻¹. The most significant correlations between SIF and physical measures of crop growth occurred at the AISA aircraft observation level (Table 3) where correlation coefficient ranging from 0.73 to 0.79 were reported for SIF spectral sensing of leaf C:N and crop yield. Similar trends were observed but relationships were not as strong between canopy observations and physical measures of crop growth. The highest association was achieved between the SIF_{RFR} and crop yield (R = -0.79). Significant relationships were not observed between SIF₆₈₈ and physical measures of crop growth. ANOVA_{LSD0.05} analysis applied to the ASD canopy and AISA FLD SIF₇₆₀ retrievals indicated values for the two N fertilization rates ≥ 140 kg N/ha were similar, while significant decreases were obtained for treatments ≤ 70 kg N/ha while SIF_{RFR} retrieved from AISA observations exhibited superior performance differentiating all four fertilization rates with a minimum significant index difference of 0.07 (Table 4c).

4.2 Diurnal Observations

Leaf A_{net} was measured over a 10 hr period with the leaf orientation adjusted to track sun position and maintain direct illumination. The diurnal variation in PAR ranged from 400 to 2400 $\mu\text{mol m}^{-2} \text{s}^{-1}$ which was the primary driving force producing a range of A_{net} values from 5 to 40 $\mu\text{mol CO}_2 \text{m}^{-2} \text{s}^{-1}$ (Fig. 3a). Sudden drops in PAR and A_{net} occurred for brief periods during mid-day cloud passes. LUE exhibited a rapid decrease in the early morning and a rapid rise in the late afternoon as PAR levels decreased below 1200 $\mu\text{mol m}^{-2} \text{s}^{-1}$. Otherwise, the diurnal response for LUE could be described as parabolic peaking at solar noon at a value of 0.28 $\mu\text{g C m}^{-2} \text{s}^{-1}$ (Fig. 3b). The response of the red-edge derivative spectral index D_{max}/D_{744} and the simple reflectance ratio R_{740}/R_{720} both exhibited consistent diurnal quadratic associations with regression coefficients of 0.83 and 0.70, respectively (Fig. 3c & 3d). The D_{max}/D_{744} index started at a value of 5.5 in the morning then decreased by 30% towards midday then recovered to its original value by evening. R_{740}/R_{720} exhibited less dynamic range and presented an inverse trend starting at 1.18 and increasing by only 3% at mid day then recovering to its original value by evening. These trends indicate significant diurnal patterns exist in red-edge spectral indices that are reversible and most likely associated with photochemical responses to changing light environment. Significant diurnal variations in band depth were also observed for the Fraunhofer absorption features reinforcing the need for simultaneous reference measurements to obtain accurate F retrievals.

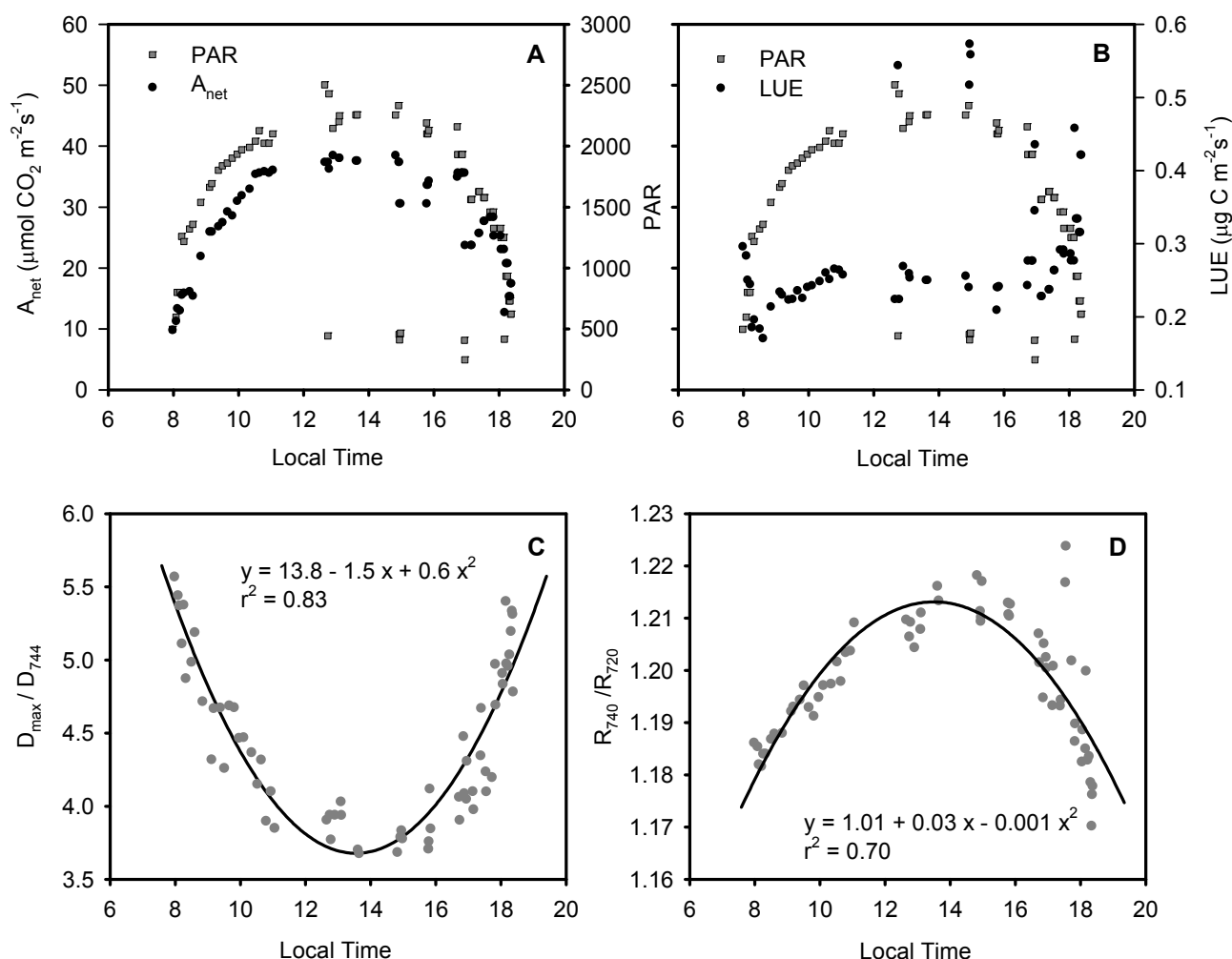


Fig. 3. Diurnal profile of *in situ* corn leaf photosynthetic gas exchange (A) and photosynthetic light use efficiency (B) with PAR levels displayed on the middle axis in units of $\mu\text{mol m}^{-2} \text{s}^{-1}$. Diurnal profiles are displayed of *in situ* adaxial corn leaf red-edge derivative reflectance index (C) and a simple reflectance ratio (D).

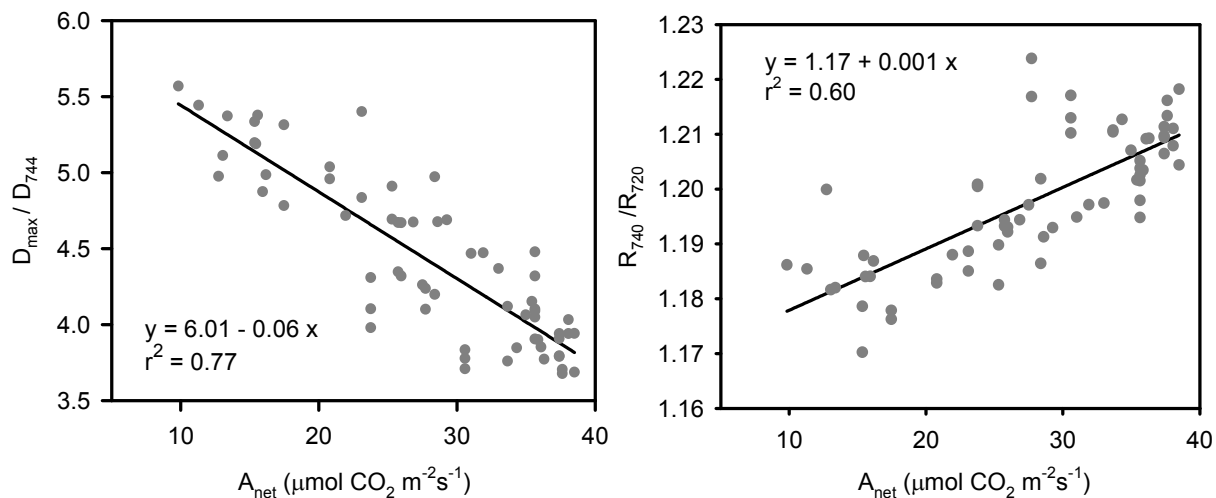


Fig. 4. Linear relationships were expressed between *in situ* leaf reflectance indices and leaf photosynthetic gas exchange. Plotted observations are for a single leaf monitored over a 10 hr period with direct solar illumination.

Of the surveyed spectral indices, the significant linear relationships between diurnal cloud free observations of leaf A_{net} and the red-edge spectral indices were noted (Fig. 4). Regression analysis indicated a higher association with the derivative reflectance ratio (D_{\max}/D_{744} , $r^2=0.77$) than the simple reflectance ratio (R_{740}/R_{720} , $r^2=0.60$). Short term cloud cover (< 15 min) did not significantly impact spectral indices but were reflected in significant drops in A_{net} . A total of five days of diurnal observations were collected on different leaves, each indicating a similar linear trend with a different slope most likely associated with leaf to leaf variation in pigment content.

4.5 Spatial analysis of crop condition

The ND_{705} and D_{730}/D_{705} R images with spatial extent covering the N experiment site at OPE3 along with kriged yield monitor data in a 2 m grid are shown in Figure 5. The N treatment plots are delineated with a white vector overlay on the geo-coded raster images. Here, spatial associations are evident between the two R indexes and yield monitor data with variation induced by N application rate visually apparent with color bars at the bottom of each panel depicting the magnitude of variation, where black is associated with low and yellow indicating high index or yield values. Within-plot variation is observed, with high and low performing areas being attributed to variable soil and hydrological properties. Overall, the low N application rates are evidenced by blue-green hues while the high N application rates are indicated by red-yellow hues.

The relationship between LUE and ASD leaf, ASD canopy, AISA aircraft R indexes D_{730}/D_{705} and ND_{705} were further explored in Figure 6. The scatter plots to the left indicate the association between multiple years of leaf R indices and corresponding *in situ* LUE measurements ($n=265$). The scatter plots in the center show the association between ASD canopy R indices and canopy LUE ($n=265$). The scatter plots to the right indicate the association between aircraft (AISA 2004, $n=60$ pixels) R indices to canopy LUE. A curvilinear association between LUE and the derivative ratio D_{730}/D_{705} was expressed at all three observation levels with index values closer to 1 for low performing areas of the field and 4 for areas with high LUE with correlation coefficients ranging from $0.74 < r < 0.79$. The relationship between ND_{705} index and LUE appears to be more linear, with correlation coefficients ranging from $0.75 < r < 0.80$. These observations imply a significant relationship to LUE for these early to mid-day R indices which were remotely observed from a corn canopy in the early reproductive growth phases.

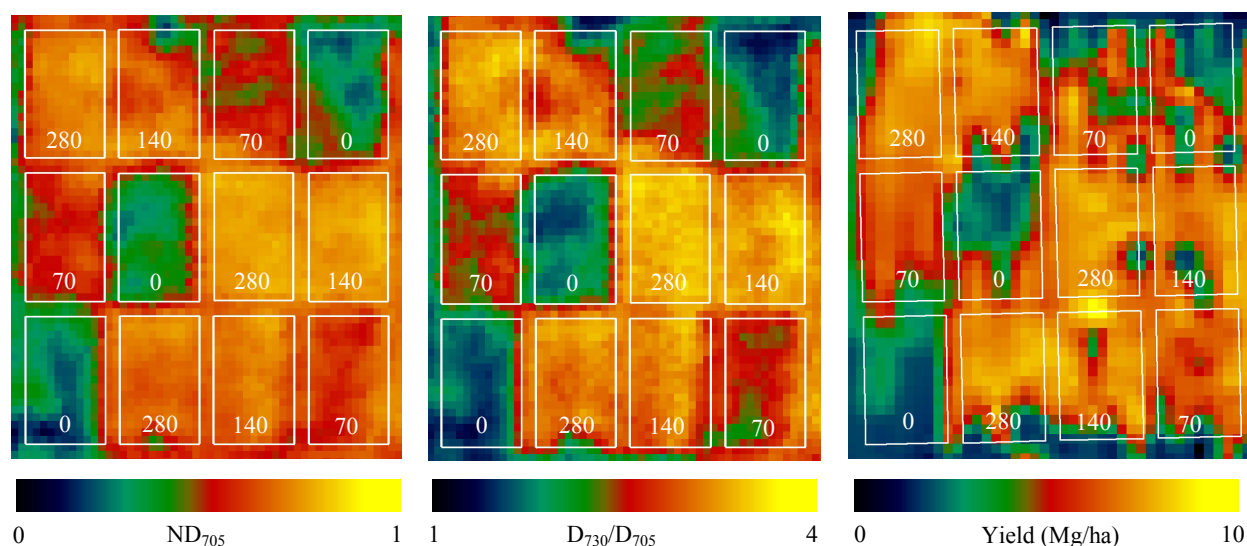


Fig. 5. Reflectance normalized difference (left) and reflectance derivative ratio (middle) spectral indices along with yield monitor data (right) over the OPE field site from AISA 2004 multispectral imagery.

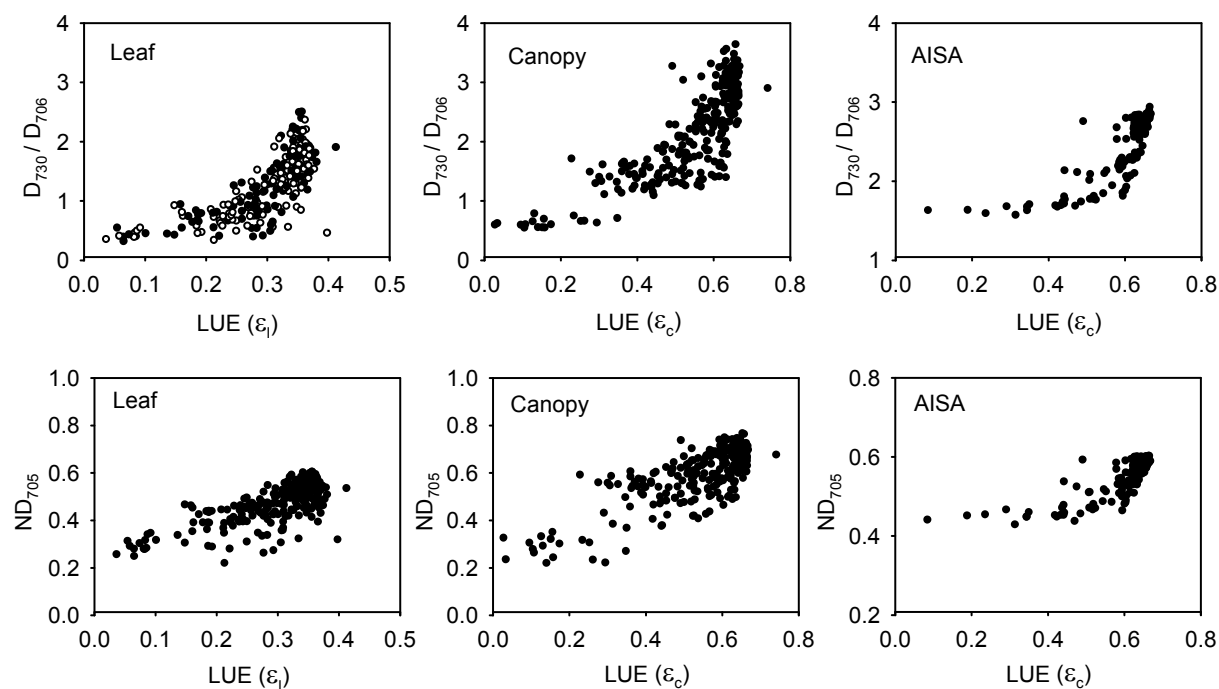


Fig. 6. Reflectance derivative ratio (top) and reflectance normalized difference (bottom) spectral indices at three observation levels versus leaf (l) or canopy (c) light use efficiency (LUE).

5. DISCUSSION

High spectral resolution R data have been demonstrated to provide significant improvement over the broadband indices for detection of differences in vegetation physiology. Further relationships between R and vegetative growth parameters have also been achieved with several derivative leaf R indices^[5]. In this study, the impact of SIF contributing to the red-edge R was apparent. Preliminary findings also suggest strong relationships exist between derivative R spectral indices and plant growth parameters. The spectral sampling resolution of the AISA instrument was not sufficient to accurately identify the wavelength position of D_{\max} or identify a significant red-edge shift in N limiting environments. However, shifts were observed in continuous sampling of the ASD instrument and leaf and canopy levels, reinforcing the importance of contiguous spectral sampling for applications involving derivative spectroscopy. The recent advances in airborne hyperspectral imaging systems (eg., AISA EAGLE & Hawk) along with the steady improvement of the AVIRIS instrument have made it possible to obtain high resolution spatial and full range visible to short-wave infrared spectral information that should be further employed to explore the impact of N availability on vegetative C uptake in both agricultural and natural ecosystems.

Here we have successfully demonstrated the extraction of SIF information from canopy R and established relationships among R and F features to crop growth and condition. The four N groups were discriminated for field corn using either passive SIF_{RFR} or R ratio indices. The reported F intensities in the O_2 bands are for near-ground observation. Absorptions by atmospheric O_2 will increasingly attenuate the F signal with sensor altitude. At orbital observation levels, this could negate the advantages of broadband O_2 features and favor the narrowband interferometers^[2]. The next logical step in these investigations is to use these summary parameters to project top-of-canopy SIF emissions to the top of atmosphere. Further studies are need with radiative transfer models to estimate the atmospheric effects on signal transmittance at orbital altitudes.

6. CONCLUSIONS

Corn crops are among the highest consumers of N fertilizers in the United States and a rapid quantitative measure of N status for this crop would prove useful to many farming systems where substantial investments are made in the application of N fertilizers. A rapid non-destructive assessment of leaf N would be useful in determining problem spots in fields where organic or chemical supplements may improve soil fertility and crop yield while reducing the potential for contamination of surface and ground waters. The findings from this study identified several well performing spectral bio-indices, which could be calculated from continuous field acquired spectra or multi-spectral AISA aircraft imagery, for the assessment of canopy N. These studies are critical to define the optimal narrow band information required for monitoring ecosystem health from space.

A number of significant relationships were evident in both reflectance and SIF indices to the biophysical changes in corn induced by varying N application rates. The FLD principle was successfully applied to canopy R spectra and AISA imagery to discriminate the relatively weak *in situ* vegetation F in-fill of the telluric O_2 bands that fall within the SIF region. From this investigation we conclude that valuable SIF information can be extracted from high-resolution reflectance data and supply useful information for modeling N use for carbon sequestration by vegetation. Results presented here indicate significant relationships exist between hyperspectral R derivative indices and FLD narrow band indices to C related vegetation parameters. These results advocate the application of hyperspectral sensors for remotely monitoring carbon cycle dynamics in terrestrial ecosystems.

REFERENCES

- [1] Gitelson, A. A., Viña, A., Verma, S. B., Rundquist, D. C., Arkebauer, T. J., Keydan, G., Leavitt, B., Ciganda, V., Burba, G. G., and Suyker, A. E., "Relationship between gross primary production and chlorophyll content in crops: Implications for the synoptic monitoring of vegetation productivity," J. Geophys. Res., 111 (2006).
- [2] Corp, L.A., Middleton, E.M., McMurtrey, J.E., Campbell, P.K.E., and Butcher, L.M., "Fluorescence sensing techniques for vegetation assessment," Applied Optics, 45(5): 1023-1033 (2006).
- [3] Freedman, A., Cavender-Bares, J., Kebabian, P., Bhaskar, R., Scott, H., and Bazzaz, F., "Remote sensing of solar-excited plant fluorescence as a measure of photosynthetic rate," Photosynthetica, 40/1, 127-132 (2002).

- [4] Liu, L., Zhang, Y., Wang, J., and Zhao, C., "Detecting solar-induced chlorophyll fluorescence from field radiance spectra based on Fraunhofer line principle," *IEEE Trans. Geosci. Remote Sens.*, 43/4, 827-832, (2005).
- [5] Middleton, E.M., Corp, L.A., and Campbell, P.K.E., "Comparison of measurements and FluorMOD simulations for solar induced chlorophyll fluorescence and reflectance of a corn crop under nitrogen treatments," *International Journal of Remote Sensing*, 29(17), 5193-5213 (2008).
- [6] Moya, I., Camenen, L., Fvain, S., Goulas, Y., Cerovic, Z., Latouche, G., Flexas, J., and Ounis, A., "A new instrument for passive remote sensing 1. Measurements of sunlight-induced chlorophyll fluorescence," *Remote Sensing of Environment*, 91, 186-197, (2004).
- [7] Zarco-Tejada P.J., Berni, J.A.J., Suárez, L., Sepulcre-Cantó, G., Morales, F., Miller, J.R., "Imaging chlorophyll fluorescence with an airborne narrow-band multispectral camera for vegetation stress detection," *Remote Sensing of Environment*, 113, 1262-1275 (2009).
- [8] Bausch, W. C., and Duke, H. R., "Remote sensing of plant nitrogen status in corn," *Transactions of the ASAE*, 39, 1869-1875, (1996).
- [9] Schlemmer, M. R., "Remotely measuring chlorophyll content in corn leaves with differing nitrogen levels and relative water content," *Agronomy Journal*, 97, 106-112 (2005).
- [10] Zhao, D. H., "Hyperspectral characteristic analysis of a developing cotton canopy under different nitrogen treatments," *Agronomie*, 24, 463-471 (2004).
- [11] Ayala-Silva, T., and Beyl, C. A., "Changes in spectral reflectance of wheat leaves in response to specific macronutrient deficiency," in *Space Life Sciences: Ground-Based Iron-Ion Biology and Physics, Including Shielding*, edited, pp. 305-317 (2005).
- [12] Asner, G. P., and Vitousek, P. M., "Remote analysis of biological invasion and biogeochemical change," *Proceedings of the National Academy of Sciences of the United States Of America*, 102, 4383-4386 (2005).
- [13] Varlet-Grancher, C., "Caractérisation et évolution de la structure d'un couvert végétal de canne à sucre," *Annales Agronomiques*, 31, 1-26 (1980).
- [14] Plascyk, J., "The MKII Fraunhofer line discriminator (FLD-II) for airborne and orbital remote sensing of solar-stimulated luminescence," *Opt. Eng.* 14, 339-346 (1975).
- [15] Meroni M., Picchi V., Rossini M., Cogliati S., Panigada C., Nali C., Lorenzini G., & Colombo R., "Leaf level early assessment of ozone injuries by passive fluorescence and PRI," *International Journal of Remote Sensing*, 29 (17), 5409-5422 (2008).
- [16] Meroni M. & Colombo R., "Leaf level detection of solar induced chlorophyll fluorescence by means of a subnanometer resolution spectroradiometer," *Remote Sensing of Environment*. 103-4: 438-448 (2006).
- [17] Gitelson, A.A., and Merzlyak, M. N., "Non-destructive assessment of chlorophyll, carotenoid and anthocyanin content in higher plant leaves: Principles and algorithms," *Remote Sensing for Agriculture and the Environment* (S. Stamatiadis, J.M. Lynch, J.S. Schepers Eds.). Greece, Ella, 2004, 78-94 (2004).
- [18] Filella, I., & Peñuelas, J., "The red edge position and shape as indicators of plant chlorophyll content, biomass and hydric status," *International Journal of Remote Sensing*, 15(7), 1459-1470 (1994).
- [19] Curran, P. J., "Remote-Sensing Of Foliar Chemistry," *Remote Sensing Of Environment*, 30, 271-278 (1989).
- [20] Huete, A., Didan, K., Miura, T., Rodriguez, E. P., Gao, X., & Ferreira, L. G., "Overview of the radiometric and biophysical performance of the MODIS vegetation indices," *Remote Sens. of Environ.*, 83, 195-213 (2002).
- [21] Sims D.A., and Gamon J.A., "Relationship between leaf pigment content and spectral reflectance across a wide range species, leaf structures and development stages," *Remote Sens. Environ.* 81: 337-354 (2002).
- [22] Gamon, J.A., Peuelas, J. and Field, C.B., "A narrow-wavelength spectral index that tracks diurnal changes in photosynthetic efficiency," *Remote Sens. of Environ.*, 41: 35-44 (1992).
- [23] Vogelmann, J.E., Rock, B.N. and Moss, D.M., "Red-edge spectral measurements in sugar maple leaves," *Int. J. Remote Sens.*, 14(8): 1563-1575 (1993).